Polímeros
ISSN 1678-5169 (Online)

https://doi.org/10.1590/0104-1428.20250057

ORIGINAL ARTICLE

Mechanical performance of biobased polyurethane composites reinforced with treated sisal fibers

Bruno Targino de Oliveira[1]*, Renata Martins Parreira[1]

[1]Mestrado Profissional em Materiais, Centro Universitário de Volta Redonda – UniFOA, Volta Redonda, RJ, Brasil

**bruno_targ@hotmail.com*

Abstract

This study investigates the mechanical behavior of biobased polyurethane (PU) composites reinforced with chemically treated sisal fibers. Two composites were fabricated: one reinforced with sisal fibers treated in a 10% NaOH solution and the other with fibers treated in a 10% $Al(OH)_3$ solution. The novelty of this work resides in comparing how each treatment affects tensile performance and fracture characteristics. Tensile tests were conducted following ASTM D3039, and fracture surfaces were analyzed by scanning electron microscopy (SEM). The composite reinforced with $Al(OH)_3$-treated fibers exhibited the highest tensile strength (15.14 MPa), followed by the NaOH-treated composite (14.09 MPa), both outperforming neat PU (6.46 MPa). SEM revealed mixed fracture modes, indicating improved fiber–matrix adhesion in treated systems. Results confirm that chemical treatment significantly enhances the mechanical properties of PU–sisal composites. Among the methods studied, $Al(OH)_3$ treatment yielded the most favorable performance, highlighting the potential of treated fibers for sustainable high-performance composites.

Keywords: *biobased polyurethane, mechanical properties, natural fiber composite, sisal fiber, tensile strength.*

Data Availability: All data supporting the findings of this study are available from the corresponding author upon request.

How to cite: Oliveira, B. T., & Parreira, R. M. (2026). Mechanical performance of biobased polyurethane composites reinforced with treated sisal fibers. *Polímeros: Ciência e Tecnologia*, *36*(1), e20260004. https://doi.org/10.1590/0104-1428.20250057

1. Introduction

The growing demand for environmentally sustainable materials has stimulated the development of polymer composites reinforced with natural fibers[1,2]. These biocomposites combine the advantages of polymers derived from renewable resources with the reinforcing potential of lignocellulosic fibers, offering an attractive alternative to synthetic composites based on glass or carbon fibers[3]. Applications in the automotive, packaging, and construction industries have particularly benefited from this trend, where lightweight structures, reduced environmental footprint, and adequate mechanical performance are required[4,5].

Several natural fibers, such as hemp, flax, jute, curauá, and sisal, have been extensively studied as reinforcements in polymer matrices[6-8]. Their main advantages include low density, biodegradability, and favorable tensile properties compared to other low-cost reinforcements. However, their hydrophilic nature and the presence of amorphous constituents (hemicellulose and lignin) hinder interfacial adhesion with hydrophobic polymer matrices, reducing stress transfer efficiency and compromising performance[9]. Therefore, surface modification of fibers through chemical treatments has been widely investigated to improve fiber–matrix compatibility[10-12].

In this study, sisal fibers were chosen as reinforcement due to their wide availability in Brazil, low cost, and socioeconomic importance. Brazil is one of the largest global producers of sisal, and its agricultural chain is already established, which ensures both accessibility and reproducibility of results[13]. Compared with hemp and flax, more common in European contexts, sisal represents a regionally relevant reinforcement with competitive mechanical properties, including high specific stiffness and satisfactory thermal resistance[14]. These characteristics, combined with its abundance, make sisal particularly attractive for developing sustainable composites in the Brazilian industrial scenario.

To enhance adhesion and improve load transfer efficiency, chemical surface modification of natural fibers is a common approach. Alkaline treatment with sodium hydroxide (NaOH) is the most widely reported method, as it removes non-cellulosic components and exposes cellulose fibrils, increasing surface roughness and enabling stronger interfacial bonding[15,16]. In this work, NaOH treatment was adopted as a reference because it is consolidated in the literature as one of the most effective strategies for improving the tensile strength of lignocellulosic fiber composites.

In parallel, aluminum hydroxide ($Al(OH)_3$) was employed as an alternative treatment. $Al(OH)_3$ is widely recognized in polymer science as a flame-retardant additive due to its ability to release water during decomposition and form protective barriers against combustion[17]. However, its use as a direct treatment for natural fibers has been scarcely explored. Investigating its influence on fiber surface morphology and interfacial adhesion is therefore novel and provides important insights into its potential to simultaneously improve mechanical properties and contribute to fire resistance. This represents a gap in the current literature and constitutes one of the original contributions of this study.

Based on these considerations, the present work aims to investigate the mechanical performance and fracture morphology of biobased polyurethane (PU) composites reinforced with sisal fibers treated with NaOH and $Al(OH)_3$ solutions. The study compares the effects of both treatments on tensile behavior and interfacial adhesion, assessed through standardized mechanical testing and scanning electron microscopy (SEM). The findings provide new perspectives on the role of chemical treatments in developing sustainable composites with improved mechanical properties and potential multifunctional characteristics.

2. Materials and Methods

2.1 Chemical treatment of sisal fibers

The sisal fibers used in this study were supplied by the Associação dos Pequenos Agricultores do Estado da Bahia (APAEB), located in the municipality of Valente, Bahia, Brazil. The purpose of the chemical treatment was to induce structural modifications in the fibers and enhance their compatibility with the polymer matrix.

The fibers were divided into two groups and subjected to different alkaline treatments. One group was immersed in an aqueous solution of sodium hydroxide (NaOH) at 10% (w/v), and the other group in an aqueous solution of aluminum hydroxide ($Al(OH)_3$) at the same concentration. In both cases, a solution-to-fiber ratio of 1 liter per 15 grams of fiber was adopted, following the procedure described by Merlini et al.[13].

The fibers remained immersed in the solutions for 1 hour at room temperature. After this period, they were rinsed with distilled water until the rinse water reached approximately neutral pH (≈7). The fibers were then dried in a forced-air oven at 100 °C for 3 hours and subsequently stored at room temperature until composite fabrication. The sequence of steps involved in the alkaline treatment process is illustrated in the treatment flow diagram (see Figure 1), including fiber preparation and chemical immersion.

Figure 1. Sequential stages of the sisal fiber alkaline treatment process: (a) weighing of raw fibers; (b) temperature monitoring of water; (c) washing of fibers in distilled water; (d) weighing of aluminum hydroxide; (e) fiber immersion in $Al(OH)_3$; (f) fiber immersion in NaOH.

2.2 Fabrication of the composites

The production of the composites was carried out using biobased polyurethane (PU) resin and chemically treated sisal fibers as the main components. The process employed a 0.3 mm silicone release sheet, 3 mm acrylic plates, a circular cutter, a precision digital scale, and the resin system supplied by Kehl Ind. e Com. Ltda – ME.

After chemical treatment, the sisal fibers were manually cut to approximately 60 mm in length, following the methodology proposed by Angrizani et al.[18], with the aim of reducing void formation and improving fiber dispersion. A fiber content corresponding to 35 wt% relative to the mass of the polyurethane resin was used, with the PU mass kept constant. Thus, the fibers were added as reinforcement rather than as matrix replacement.

Molding was performed in an acrylic mold with dimensions of 90 × 265 × 3 mm, designed to ensure proper shaping, facilitate demolding, and standardize specimen dimensions (see Figure 2). The fibers were randomly arranged inside the mold. To limit uncontrolled expansion of the polyurethane, a blind acrylic plate was placed on top of the mold and a static load of approximately 29.7 kg (four concrete blocks) was applied for two hours. This procedure corresponds to a controlled expansion process with static pre-compaction, rather than conventional compression molding under defined pressure. After this step, the resin was poured, the composites were cured at room temperature for 4 h, and the specimens were subsequently demolded and cut according to ASTM D3039[19] and ASTM D635 standards.

The polyurethane system was formulated using a stoichiometric 1:1 mass ratio of components A (isocyanate) and B (polyol), as recommended in the product's safety data sheet (FISPQ)[20]. An additional 15% was added to each component to compensate for material losses due to adhesion and handling. Each component was stirred individually for 5 minutes and then mechanically mixed for an additional 5 minutes, following the manufacturer's instructions. The mixing and resin preparation procedure is illustrated in the schematic diagram (see Figure 3).

The resulting PU mixture was poured directly onto the compacted fiber mat, allowing controlled expansion to ensure uniform impregnation of the reinforcement. The composite was then cured at room temperature for 4 hours. After curing, the specimens were demolded and cut according to the ASTM D3039[19] (tensile test) and ASTM D635 (horizontal flammability test) standards.

2.3 Characterization methods

To evaluate the mechanical performance of the produced composites, tensile tests were performed in accordance with ASTM D3039. Specimens were manually cut from the molded composite panels, with standard dimensions of 250 mm in length, 25 mm in width, and 3 mm in thickness[8]. A minimum of four specimens was tested for each material type: PU reinforced with NaOH-treated fibers, PU reinforced with $Al(OH)_3$-treated fibers, and neat PU.

The tensile tests were conducted using an Emic universal testing machine equipped with a 100 kN load cell, operating at a constant crosshead speed of 2 $mm \cdot min^{-1}$[19] at room temperature.

Following mechanical testing, fracture surface analysis was carried out using a benchtop scanning electron microscope (SEM), model Hitachi TM 3000. The micrographs allowed for the identification of failure mechanisms such as fiber pull-out, matrix rupture, and fiber–matrix interfacial debonding, providing morphological evidence to support the mechanical test results.

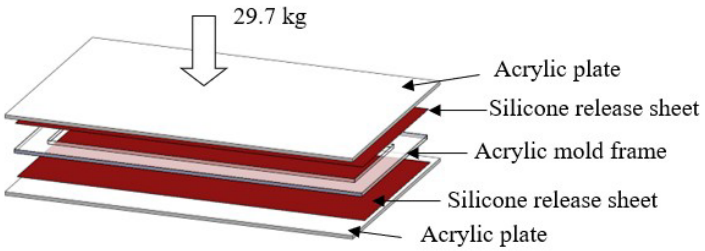

Figure 2. Schematic representation of the mold setup used for composite fabrication, showing the arrangement of silicone release sheets, acrylic mold, and applied pressure.

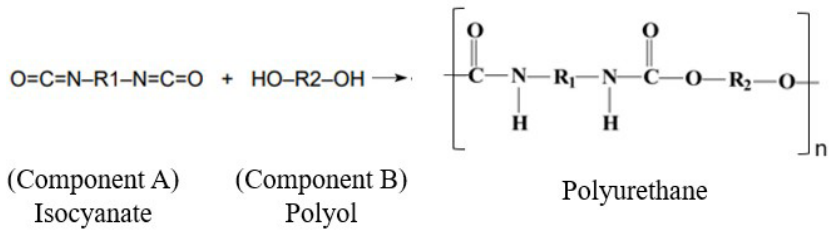

Figure 3. Schematic representation of polyurethane resin preparation: reaction between component A (isocyanate) and component B (polyol), resulting in urethane linkages and formation of the PU matrix.

3. Results and Discussions

This section presents and discusses the main results from the mechanical and morphological characterization of biobased polyurethane composites reinforced with sisal fibers treated with alkaline solutions of NaOH and $Al(OH)_3$. The tensile strength results of the composites are analyzed in comparison to neat PU, highlighting the specific contributions of each fiber treatment. Additionally, scanning electron microscopy (SEM) images of the fracture surfaces are examined to discuss the failure mechanisms observed, providing morphological insights that complement and help explain the mechanical behavior.

3.1 Tensile strength of the composites

The tensile test results for neat polyurethane (PU) and for the composites reinforced with sisal fibers treated with alkaline solutions are presented in Table 1. The neat PU exhibited an average tensile strength of 6.46 ± 0.93 MPa, an elastic modulus of 0.08 ± 0.01 GPa, and an elongation at break of 8.12 ± 0.40%.

The incorporation of chemically treated sisal fibers significantly enhanced the mechanical performance of the PU matrix. The composite reinforced with NaOH-treated fibers achieved an average tensile strength of 14.09 ± 1.24 MPa, while the composite with $Al(OH)_3$-treated fibers reached 15.14 ± 2.07 MPa, corresponding to increases of 118.11% and 134.36%, respectively, compared to neat PU.

Furthermore, the elastic modulus increased to 0.56 ± 0.04 GPa for the NaOH composite and to 0.75 ± 0.10 GPa for the $Al(OH)_3$ composite. In contrast, the elongation at break decreased to 2.51 ± 0.11% and 2.02 ± 0.22%, respectively, indicating that the fiber reinforcement increased stiffness while reducing ductility.

One-way ANOVA was conducted to evaluate the differences among the three groups (neat PU and both fiber-reinforced composites). The test yielded an F-value of 26.06 and a p-value of 0.000067, demonstrating a statistically significant difference among groups ($p < 0.05$). The F statistic represents the ratio of variance between groups to variance within groups, while the p-value corresponds to the probability, under the null hypothesis of equal means, of obtaining such an F-value. Post-hoc Tukey tests confirmed that both NaOH- and $Al(OH)_3$-treated composites were significantly different from neat PU, with the $Al(OH)_3$ treatment yielding the highest mean strength.

It is important to note that this study did not include a composite reinforced with untreated sisal fibers, due to the limited amount of resin available for processing. Therefore, while the present results demonstrate that fiber treatments are associated with improved mechanical performance compared to neat PU, further experiments including untreated sisal as a control will be necessary to directly quantify the incremental effect of chemical modifications. Nevertheless, SEM analysis provides supporting evidence that the improvements observed are consistent with enhanced fiber–matrix interfacial bonding promoted by the treatments.

The revised stress–strain curves (see Figure 4) emphasize the mechanical advantages of the reinforced systems over neat PU. Both composites exhibit steeper initial slopes, indicating increased stiffness. After the peak stress, the curves show a sharp drop, characteristic of brittle fracture behavior with limited post-peak deformation. The composite reinforced with $Al(OH)_3$-treated fibers displays the steepest initial slope, reflecting its superior elastic modulus. In contrast, the neat PU shows an extended region of nearly constant stress with increasing strain, which in some specimens was attributed to grip slippage artifacts; these curves were discarded and repeated to ensure reliable elongation-at-break data.

These results are in line with the findings of Sencadas et al.[21], Kilinç et al.[16], and Liu et al.[17] , who reported increased tensile strength in composites reinforced with chemically treated sisal fibers. The values obtained in this study are consistent with those previously reported, considering the variability in fiber treatments and matrix structures.

3.2 Morphological analysis of the composites

The fracture morphology of the test specimens was analyzed by scanning electron microscopy (SEM) to better understand the failure mechanisms associated with the mechanical performance observed.

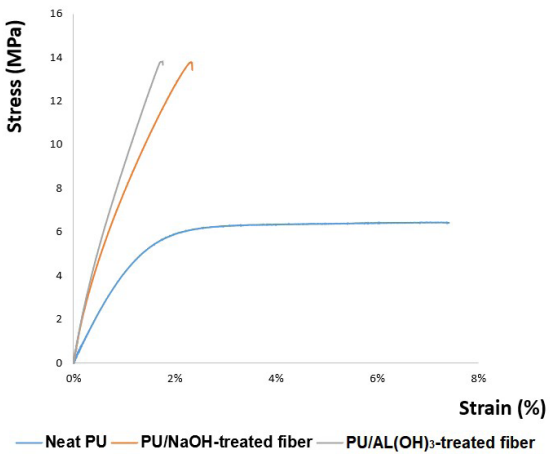

Figure 4. Stress–strain curves of neat polyurethane (PU) and composites reinforced with sisal fibers treated with NaOH and $Al(OH)_3$.

Table 1. Mechanical properties of neat polyurethane (PU) and composites reinforced with chemically treated sisal fibers.

Material	Tensile Strength (MPa)	Elastic Modulus (GPa)	Elongation at Break (%)
Neat Pu	6,46 ± 0.93	0.08 ± 0.01	8,12 ± 0.40%
Composite NaOH-treated fiber	14,09 ± 1,24	0.56 ± 0.04	2,51 ± 0.11%
Composite $Al(OH)_3$-treated fiber	15,14 ± 2,07	0.75 ± 0.1	2,02 ± 0.22%

The SEM image of the fracture surface of neat polyurethane (PU) revealed a highly porous structure with numerous air bubbles and voids of varying sizes, distributed relatively homogeneously throughout the matrix (see Figure 5). While this morphology may reflect good uniformity during molding, it also suggests the presence of stress concentration zones that can negatively affect mechanical strength. The smooth edges of the pores and the presence of visible cracks support the hypothesis of brittle fracture behavior, consistent with findings reported in the literature[21].

The fracture surface of the composite reinforced with sisal fibers treated with NaOH reveals several distinct morphological features (see Figure 6). Voids are dispersed throughout the matrix, likely formed during the curing process due to the entrapment of volatile gases. These imperfections compromise the material's homogeneity and may contribute to reduced tensile strength.

A reasonably homogeneous distribution of fibers with random orientations is also observed. While some fibers are well embedded in the matrix, others exhibit partial pull-out, indicating areas of weak interfacial adhesion. However, regions with visible residual matrix adhered to the fiber surfaces suggest localized mechanical interlocking, which may contribute positively to load transfer in certain zones.

This interpretation is further supported by the SEM analysis (see Figure 7), which highlights the occurrence of fiber pull-out, where fibers are partially extracted from the matrix during fracture. This behavior is typically associated with insufficient interfacial adhesion, potentially resulting from physical or chemical incompatibilities between the fiber and the matrix. At the same time, some fibers appear to have fractured rather than being pulled out (see Figure 7a), suggesting that effective stress transfer occurred from the matrix to the reinforcement. This combination of pull-out

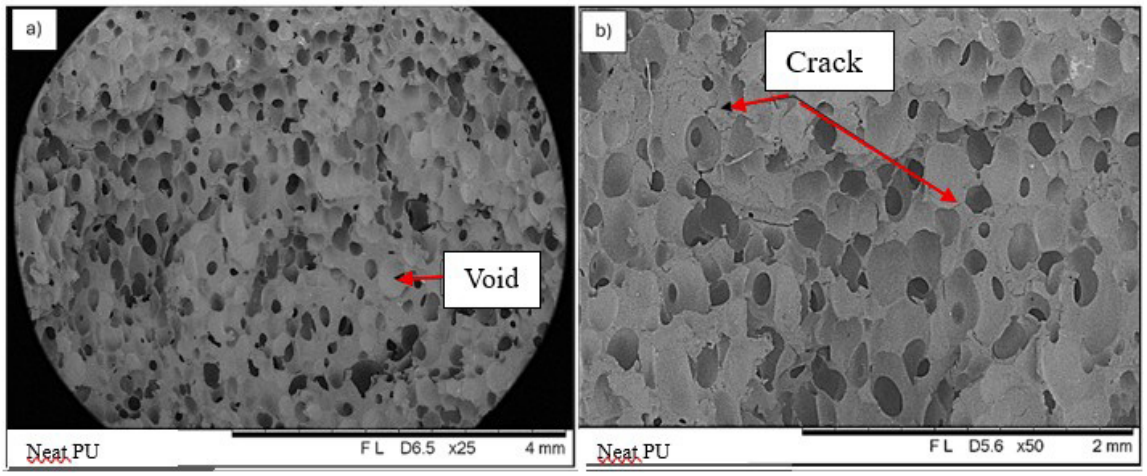

Figure 5. SEM micrographs of the fracture surface of neat polyurethane (PU): (a) Porous morphology with distributed air bubbles (magnification: 25×); (b) Evidence of surface cracks (fissures), indicative of brittle fracture (magnification: 50×).

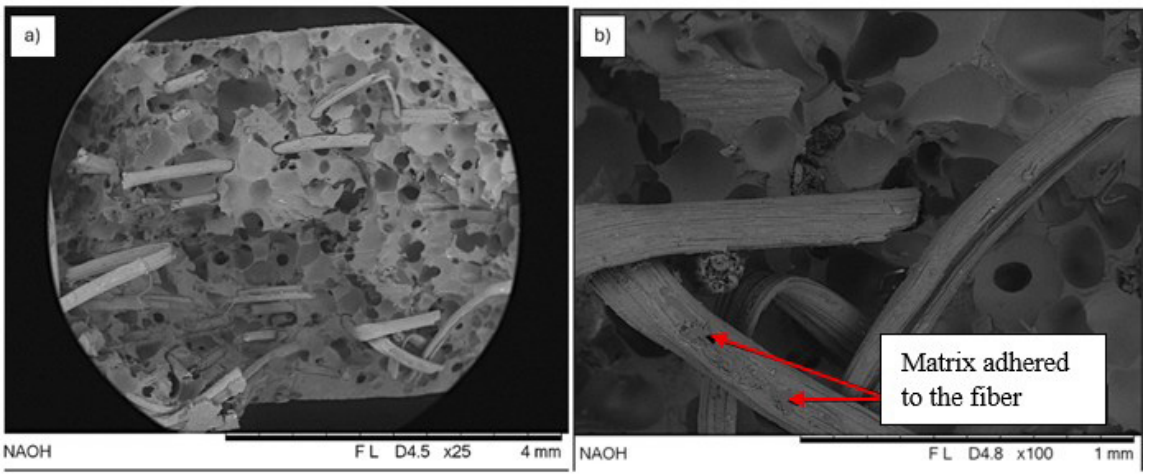

Figure 6. SEM micrographs of the fracture surface of the PU composite reinforced with NaOH-treated sisal fibers: (a) Voids and randomly oriented fibers dispersed in the matrix (25×); (b) Fiber–matrix interface showing regions of partial adhesion and matrix residue.

and fiber fracture explains the higher tensile strength and stiffness of the $Al(OH)_3$-treated composite, while its lower elongation at break indicates that these gains were accompanied by increased brittleness compared to the NaOH-treated system.

A transverse fracture of the NaOH-treated sisal fiber reveals important characteristics of the failure mechanism (see Figure 8). The fractured surfaces appear rough and inclined, with exposed microfibrillar layers, which are indicative of a shear-dominated failure. This morphology suggests that the fibers were able to absorb energy during loading and only fractured after reaching their tensile limit. Additionally, the presence of residual matrix adhered to the fiber surface reinforces the evidence of effective fiber–matrix interfacial bonding.

The fracture morphology of the composite reinforced with $Al(OH)_3$-treated fibers reveals notable differences when compared to the NaOH-treated system (see Figure 9). Fewer voids are observed throughout the matrix, suggesting greater homogeneity and more efficient stress transfer between the matrix and the fibers. Although the fiber pull-out phenomenon is still present, it appears less pronounced, indicating improved interfacial bonding in certain regions. These microstructural features explain the higher tensile strength and stiffness of the $Al(OH)_3$ composite; however, they are also consistent with its lower elongation at break, reflecting a more brittle behavior than the NaOH-treated system.

Additional morphological details of the $Al(OH)_3$-treated fiber composite are presented (Figure 10). Partial separation of fiber bundles and the orderly detachment of layers are observed, indicating a shear-dominated failure mechanism. The progressive delamination of fiber layers suggests that the treatment preserved the hierarchical structure of the fibers, contributing to efficient load transfer and the higher stiffness observed. However, in agreement with the mechanical results, the overall composite exhibited lower elongation

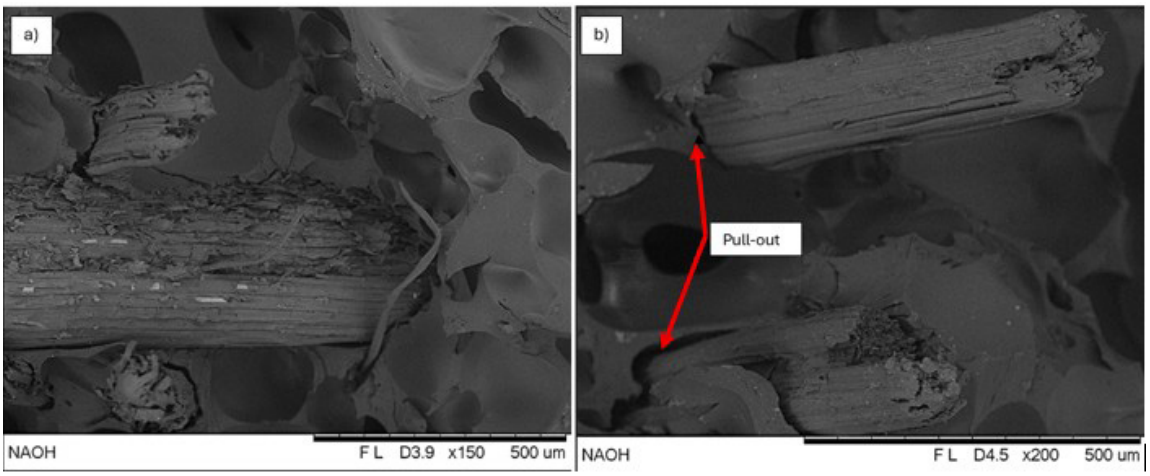

Figure 7. SEM micrographs of the PU/NaOH composite fracture surface highlighting interfacial failure mechanisms: (a) Fractured fiber indicating stress transfer from the matrix; (b) Evidence of fiber pull-out, suggesting regions of weak fiber–matrix adhesion.

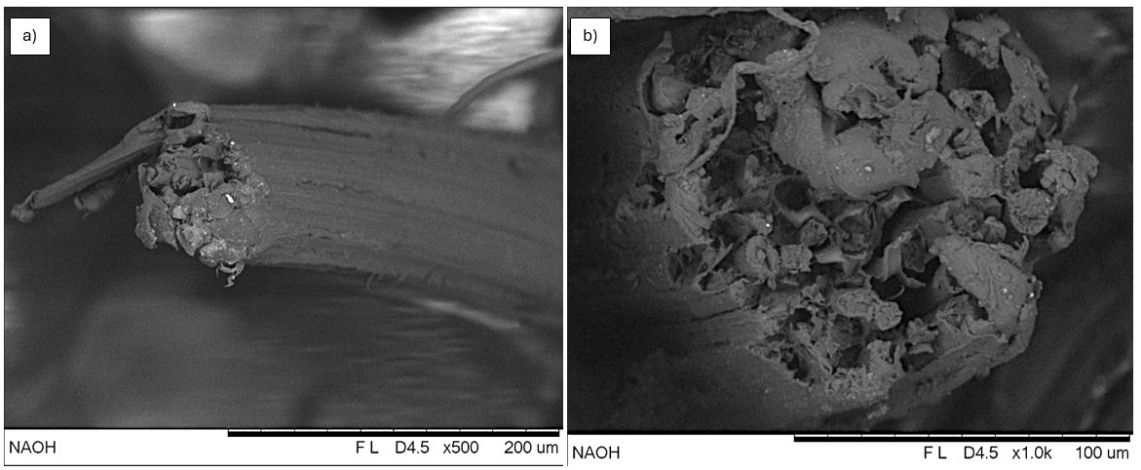

Figure 8. SEM micrographs of fractured NaOH-treated sisal fibers: (a) Rough and inclined fracture surface with signs of shear failure and residual matrix; (b) Transverse fiber rupture exposing microfibrillar layers, indicating energy absorption before failure.

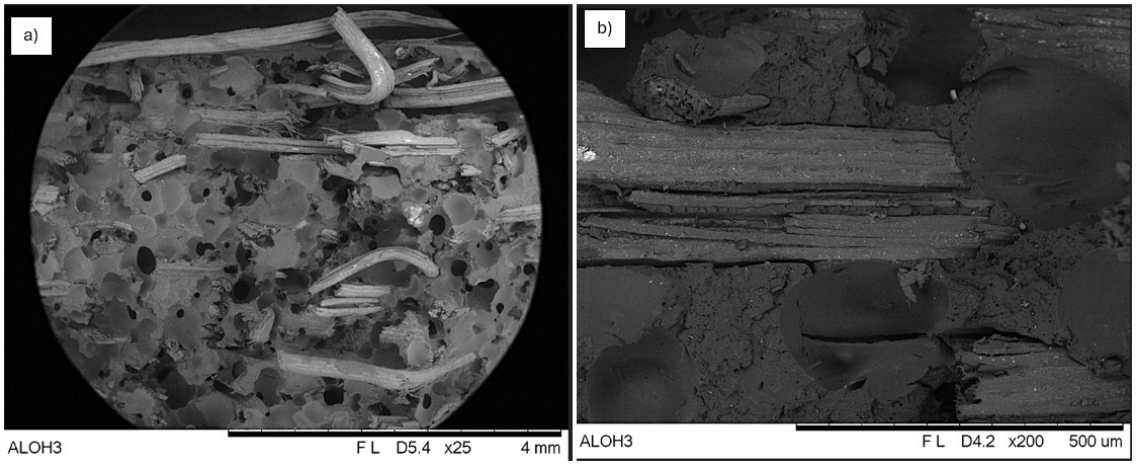

Figure 9. SEM micrographs of the PU composite reinforced with $Al(OH)_3$-treated sisal fibers: (a) Fracture surface with reduced void content, indicating improved matrix homogeneity (25×); (b) Fiber pull-out observed at the fracture interface, suggesting moderate interfacial adhesion (200×).

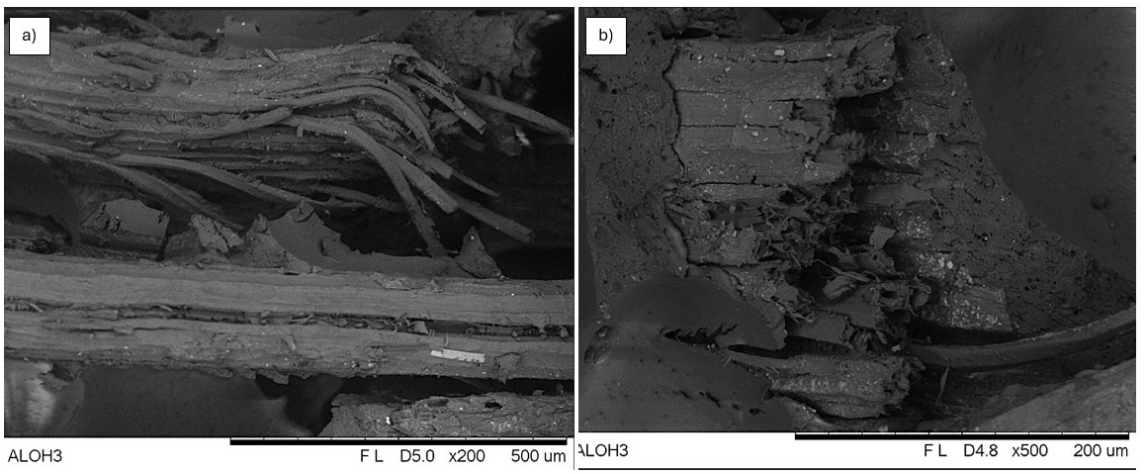

Figure 10. SEM micrographs of the PU/$Al(OH)_3$ composite: (a) Gradual fiber bundle separation with shear fracture features (200×); (b) Delaminated fiber with residual particles on the surface (500×).

at break, reflecting a more brittle behavior compared to the NaOH-treated system. Furthermore, small bright regions (white spots) visible on the fiber surface may correspond to residual aluminum hydroxide particles. These residues could potentially enhance flame-retardant properties and improve fiber–matrix bonding by forming a protective layer or enhancing interfacial compatibility[16].

3.3 Correlation between morphology and mechanical performance

The correlation between the tensile properties and the fracture morphology reveals clear links between microstructure and performance. In neat PU, the low tensile strength (6.46 MPa) can be directly related to its highly porous structure, as evidenced in Figure 5. The presence of voids and entrapped air bubbles acted as stress concentrators, reducing the effective cross-section of the material and favoring the premature nucleation of cracks. This microstructural condition limited the capacity for plastic deformation and promoted brittle fracture, which was also confirmed by the smooth pore edges and cracks observed under SEM, in agreement with previous studies[21].

When sisal fibers were incorporated, the mechanical performance improved substantially. The NaOH-treated composite reached 14.09 MPa, while the $Al(OH)_3$-treated composite achieved 15.14 MPa, both significantly higher than neat PU. These results highlight the role of the fibers as effective reinforcements and show the importance of the fiber–matrix interface in governing stress transfer. The higher elastic modulus values measured for the composites confirm that the inclusion of fibers restricted matrix deformation, producing stiffer materials.

The micrographs of the NaOH-reinforced composite (Figures 6-8) illustrate this effect. Although voids remained, reflecting imperfections from curing, the fibers appeared relatively well distributed in random orientations. Partial pull-out was observed in some regions, indicating areas of weaker adhesion, but several fibers retained residual matrix on their surfaces, suggesting localized interfacial bonding. This morphology explains the intermediate performance of this composite: tensile strength and modulus clearly superior to neat PU, while preserving slightly higher elongation at break compared with the $Al(OH)_3$ composite.

The $Al(OH)_3$-treated composite (Figures 9 and 10) displayed a distinct morphology, with fewer voids and more cohesive fiber–matrix integration. Shear-type fractures and fibrillar bundles suggested efficient load transfer and stronger interfacial bonding. Bright spots observed on fiber surfaces were attributed to aluminum hydroxide residues, which may contribute both to flame retardancy and to improved compatibility at the interface[10]. These structural features justify the highest tensile strength (15.14 MPa) and elastic modulus (0.75 GPa) obtained. However, the reduced elongation at break confirms that the $Al(OH)_3$ composite was the most brittle system investigated, since the gains in stiffness were accompanied by a loss of deformability.

A direct comparison between the two treatments reveals a trade-off between strength, stiffness, and ductility. The NaOH-treated composite provided significant reinforcement and maintained a limited capacity for deformation, while the $Al(OH)_3$ treatment maximized stiffness and strength but produced the most brittle response. These differences reflect the distinct chemical effects of the treatments: NaOH removed amorphous constituents such as hemicellulose and lignin, increasing fiber roughness and promoting mechanical interlocking, while $Al(OH)_3$ generated surface deposits that enhanced load transfer but also reduced fiber flexibility, limiting the ability of the composite to accommodate strain.

Taken together, these results confirm that porosity, fiber–matrix adhesion, and fracture mechanisms are decisive factors in the mechanical behavior of PU–sisal composites. Both chemical treatments improved reinforcement significantly, but with different balances: $Al(OH)_3$ produced the stiffest and strongest composite, albeit the most brittle, while NaOH offered a more balanced compromise between stiffness and residual ductility. These findings emphasize that fiber treatments must be tailored to the intended application, depending on whether stiffness, strength, or toughness is the primary requirement.

4. Conclusions

This study aimed to evaluate the mechanical and morphological behavior of sustainable composites based on biobased polyurethane reinforced with sisal fibers treated with alkaline solutions of NaOH and $Al(OH)_3$. Based on the results obtained, the proposed objective was successfully achieved.

The incorporation of chemically treated fibers led to a significant enhancement in the mechanical performance of the composites, confirming the effectiveness of sisal fiber reinforcement in biopolymer matrices. The tensile strength, stiffness, and modulus values increased considerably in both reinforced systems when compared to neat polyurethane. Furthermore, the SEM-based morphological evaluation provided valuable insights into the fracture mechanisms, emphasizing the crucial role of fiber–matrix interfacial bonding.

The composite reinforced with $Al(OH)_3$-treated fibers exhibited better interfacial integration and a more uniform internal structure, resulting in the highest stiffness and tensile strength. However, these gains were accompanied by the lowest elongation at break, confirming its more brittle behavior. In contrast, the NaOH-treated composite also provided significant improvements over neat PU but retained slightly greater ductility, representing a more balanced compromise between stiffness and deformability.

Overall, the findings reinforce the viability of using chemically modified natural fibers as reinforcements in sustainable composite systems. The mechanical improvements, combined with the environmental advantages of biobased materials, support the application of these composites in engineering contexts that demand low weight, renewable sourcing, and reliable mechanical performance.

5. Author's Contribution

- **Conceptualization –** Bruno Targino de Oliveira; Renata Martins Parreira.
- **Data curation –** Bruno Targino de Oliveira; Renata Martins Parreira.
- **Formal analysis –** Bruno Targino de Oliveira.
- **Funding acquisition –** NA.
- **Investigation –** Bruno Targino de Oliveira; Renata Martins Parreira.
- **Methodology –** Bruno Targino de Oliveira; Renata Martins Parreira.
- **Project administration –** Bruno Targino de Oliveira; Renata Martins Parreira.
- **Resources –** Bruno Targino de Oliveira.
- **Software –** NA.
- **Supervision –** NA.
- **Validation –** Bruno Targino de Oliveira; Renata Martins Parreira.
- **Visualization –** Bruno Targino de Oliveira; Renata Martins Parreira.
- **Writing – original draft –** Bruno Targino de Oliveira.
- **Writing – review & editing –** Bruno Targino de Oliveira; Renata Martins Parreira.

6. Acknowledgements

The authors would like to express their gratitude to Centro Universitário de Volta Redonda (UniFOA) for providing the chemical reagents used in the fiber surface treatments and for granting access to the laboratory facilities required for the characterization experiments. They also thank Kehl Indústria e Comércio Ltda – ME for the technical support and for supplying the polyurethane resin system used in this study.

7. References

1. Mora-Murillo, L. D., Orozco-Gutiérrez, F., Vega-Baudrit, J., & González-Paz, R. J. (2017). Thermal-mechanical characterization of polyurethane rigid foams: effect of modifying bio-polyol content in isocyanate prepolymers. *Journal of Renewable Materials*, *5*(3-4), 220-230. https://doi.org/10.7569/JRM.2017.634112.
2. Ionescu, M. (2005). *Chemistry and technology of polyols for polyurethanes*. Shawbury: Rapra Technology Limited.
3. Faruk, O., Bledzki, A. K., Fink, H.-P., & Sain, M. (2012). Biocomposites reinforced with natural fibers: 2000–2010. *Progress in Polymer Science*, *37*(11), 1552-1596. https://doi.org/10.1016/j.progpolymsci.2012.04.003.
4. Yan, L., Chouw, N., & Jayaraman, K. (2014). Flax fibre and its composites – A review. *Composites. Part B, Engineering*, *56*, 296-317. https://doi.org/10.1016/j.compositesb.2013.08.014.
5. Rev, T., Wisnom, M. R., Xu, X., & Czél, G. (2022). The effect of transverse compressive stresses on tensile failure of carbon fibre/epoxy composites. *Composites. Part A, Applied Science and Manufacturing*, *156*, 106894. https://doi.org/10.1016/j.compositesa.2022.106894.
6. Monteiro, S. N., Lopes, F. P. D., Barbosa, A. P., Bevitori, A. B., Silva, I. L. A., & Costa, L. L. (2011). Natural lignocellulosic fibers as engineering materials: an overview. *Metallurgical and Materials Transactions. A, Physical Metallurgy and Materials Science*, *42*(10), 2963-2974. https://doi.org/10.1007/s11661-011-0789-6.
7. Liao, Z., Hu, Y., Shen, Y., Chen, K., Qiu, C., Yang, J., & Yang, L. (2024). Investigation into the reinforcement modification of natural plant fibers and the sustainable development of thermoplastic natural plant fiber composites. *Polymers*, *16*(24), 3568. https://doi.org/10.3390/polym16243568. PMid:39771421.
8. Fernandes, R. A. P., Silveira, P. H. P. M., Bastos, B. C., Pereira, P. S. C., Melo, V. A., Monteiro, S. N., Tapanes, N. L. C. O., & Bastos, D. C. (2022). Bio-based composites for light automotive parts: statistical analysis of mechanical properties; effect of matrix and alkali treatment in sisal fibers. *Polymers*, *14*(17), 3566. https://doi.org/10.3390/polym14173566. PMid:36080641.
9. Campos, A., Teodoro, K. B. R., Marconcini, J. M., Mattoso, L. H. C., & Martins-Franchetti, S. M. (2011). Effect of fiber treatments on properties of thermoplastic starch/polycaprolactone/sisal biocomposites. *Polímeros: Ciência e Tecnologia*, *21*(3), 217-222. https://doi.org/10.1590/S0104-14282011005000039.
10. Ichim, M., Muresan, E. I., & Codau, E. (2024). Natural-fiber-reinforced polymer composites for furniture applications: technical, ecological and economic demands. *Polymers*, *16*(22), 3113. https://doi.org/10.3390/polym16223113. PMid:39599204.
11. Thimmegowda, D. Y., Hindi, J., Markunti, G. B., & Kakunje, M. (2025). Enhancement of mechanical properties of natural fiber reinforced polymer composites using different approaches: a review. *Journal of Composites Science*, *9*(5), 220. https://doi.org/10.3390/jcs9050220.
12. Thepruttana, S., Patthanavarit, J., Hankoy, M., Kitiwan, M., Keawprak, N., & Tunthawiroon, P. (2024). Enhancement of flexural strength in fiber–cement composites through modification of sisal fiber with natural rubber latex and expanded perlite. *Buildings (Basel, Switzerland)*, *14*(4), 1067. https://doi.org/10.3390/buildings14041067.
13. Merlini, C., Soldi, V., & Barra, G. M. O. (2011). Influence of fiber surface treatment and length on physico-chemical properties of short random banana fiber-reinforced castor oil polyurethane composites. *Polymer Testing*, *30*(8), 833-840. https://doi.org/10.1016/j.polymertesting.2011.08.008.
14. Olanrewaju, O., Oladele, I. O., & Adelani, S. O. (2025). Recent advances in natural fiber reinforced metal/ceramic/polymer composites: an overview of the structure-property relationship for engineering applications. *Hybrid Advances*, *8*, 100378. https://doi.org/10.1016/j.hybadv.2025.100378.
15. Islam, S., Hasan, B., Kodrić, M., Motaleb, K. Z. M. A., Karim, F.-E., & Islam, R. (2025). Mechanical properties of hemp fiber-reinforced thermoset and thermoplastic polymer composites: a comprehensive review. *SPE Polymers*, *6*(1), e10173. https://doi.org/10.1002/pls2.10173.
16. Kılınç, A. C., Atagür, M., Özdemir, O., Şen, I., Küçükdoğan, N., Sever, K., Seydibeyoğlu, O., Sarikanat, M., & Seki, Y. (2016). Manufacturing and characterization of vine stem reinforced high density polyethylene composites. *Composites. Part B, Engineering*, *91*, 267-274. https://doi.org/10.1016/j.compositesb.2016.01.033.
17. Liu, Y., Zhang, X., Liu, J., Xing, D., Shen, H., Chen, D., & Sun, J. (2015). Superelasticity in polycrystalline Ni-Mn-Ga-Fe microwires fabricated by melt-extraction. *Materials Research*, *18*(Suppl. 1), 61-65. https://doi.org/10.1590/1516-1439.325914.
18. Angrizani, C. C., Amico, S. C., Cioffi, M. O. H., & Zattera, A. J. (2014). Influência da espessura nas propriedades mecânicas de compósitos híbridos interlaminares de curauá/vidro/poliéster. *Polímeros*, *24*(2), 184-189. https://doi.org/10.4322/polimeros.2014.063.
19. American Society for Testing and Materials - ASTM. (2017). *ASTM D3039/D3039M-17: Standard test method for tensile properties of polymer matrix composite materials*. West Conshohocken: ASTM. Retrieved in 2025, July 15, from https://www.astm.org/d3039_d3039m-17.html
20. Kehl Indústria e Comércio Ltda – ME. (2022). *FISPQ – Ficha de Informações de Segurança de Produto Químico: Sistema Poliol + Isocianato PU Vegetal*. Retrieved in 2025, July 15, from https://www.kehl.ind.br
21. Sencadas, V., Correia, D. M., Ribeiro, C., Moreira, S., Botelho, G., Gómez Ribelles, J. L., & Lanceros-Méndez, S. (2012). Physical–chemical properties of cross-linked chitosan electrospun fiber mats. *Polymer Testing*, *31*(8), 1062-1069. https://doi.org/10.1016/j.polymertesting.2012.07.010.

Received: Jul. 15, 2025
Revised: Oct. 05, 2025
Accepted: Nov. 04, 2025

Editor-in-Chief: *Sebastião V. Canevarolo*